

Surface Plasmon Polariton Mediated Multiple Toroidal Resonances in 3D Folding Metamaterials

Shengyan Yang,^{†,‡} Zhe Liu,[†] Ling Jin,[†] Wuxia Li,[†] Shuang Zhang,^{*,§} Junjie Li,^{*,†,‡,||} and Changzhi Gu^{*,†,‡,||}

[†]Beijing National Laboratory for Condensed Matter Physics, Institute of Physics, Chinese Academy of Sciences, Beijing 100190, China

[§]School of Physics and Astronomy, University of Birmingham, Birmingham B15 2TT, United Kingdom

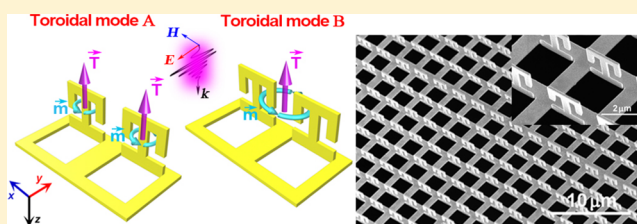
[‡]School of Physical Sciences, CAS Key Laboratory of Vacuum Physics, University of Chinese Academy of Sciences, Beijing 100049, China

^{||}Collaborative Innovation Center of Quantum Matter, Beijing, China

Supporting Information

ABSTRACT: Toroidal dipole has attracted tremendous attentions in nuclear, particle, condensed matter and material physics due to its exotic characteristics that are distinct from the fundamental electric and magnetic dipoles. Due to the very weak intensity, toroidal dipolar response is extremely difficult to be detected in natural materials. Although single dynamic toroidal dipole has recently been observed in metamaterials, simultaneous observation of multiple toroidal dipole resonances is still very challenging, and many intriguing physical phenomena associated with them have remained elusive. Here we experimentally demonstrate an approach to achieving toroidal dipole responses with high quality factors in the infrared region via surface-plasmon-polariton excitation. Implementation of this concept leads to simultaneous experimental observation of double toroidal modes in 3D metamaterial. Periodicity and angle dependent transmission measurements clearly reveal the coupling between the surface-plasmon-polariton mode and toroidal modes. Our demonstration provides a unique platform for the study of toroidal electrodynamics and various astonishing optical phenomena involving toroidal moments.

KEYWORDS: metamaterials, toroidal resonances, subwavelength optics, surface plasmon polariton, extraordinary optical transmission (EOT)



Toroidal dipole moment, first considered by Zel'dovich in 1957 to interpret the parity violation of the weak interaction in nuclear and particle physics, has been shown to complement the classical electromagnetic theory of multipole expansion.¹ Being physically distinct from the electric and magnetic dipoles that arise from a pair of charges and circulating currents respectively, the intriguing toroidal dipole is a peculiar elementary current excitation corresponding to electrical currents circulating on a surface of a gedanken torus along its meridians. Because the toroidal dipolar moment violates the symmetries of both time-inversion and space reversal operation, many intriguing properties has been theoretically predicted in solid-state physics, and its significance has been discussed for various condensed matter systems including multiferroics, molecular magnets, special macromolecules, ferroelectric, ferromagnetic materials, and so on.^{2–11} A static toroidal moment in condensed matters is manifested as a vortex distribution of head-to-tail arrangement of magnetic dipoles, and mathematically defined as $\vec{T} = \sum \vec{r}_i \times \vec{M}_i$, where \vec{M}_i is the magnetic dipole moment, \vec{r}_i is the displacement of the magnetic dipole from the toroidal center,

and i in the subscript represents the i th magnetic dipole that contributes to the toroidal moment.^{1,2,7} Magnetic dipole moments in condensed matter systems are usually produced by distinct spins or orbital momenta of the electrons, and thus, there generally exist multiple toroidal dipole modes (toroidal moments). The toroidal moments provided by different electron spins and orbital momenta generally have distinct magnitudes and orientations, which produce various exotic phenomena and effects, such as the magnetoelectric effect, enhanced nonlinear susceptibility, dichroism, and toroidal induced nonreciprocal refraction.^{2,4–7,10,11} Although the importance of static toroidal moment in particle physics and condensed matter systems has been established, not much attention has been paid to the dynamic toroidal response in electromagnetism until very recently, as it is extremely difficult to detect experimentally due to its weak response in naturally occurring materials. Therefore, to induce dominant dynamic

Received: May 26, 2017

Published: October 26, 2017

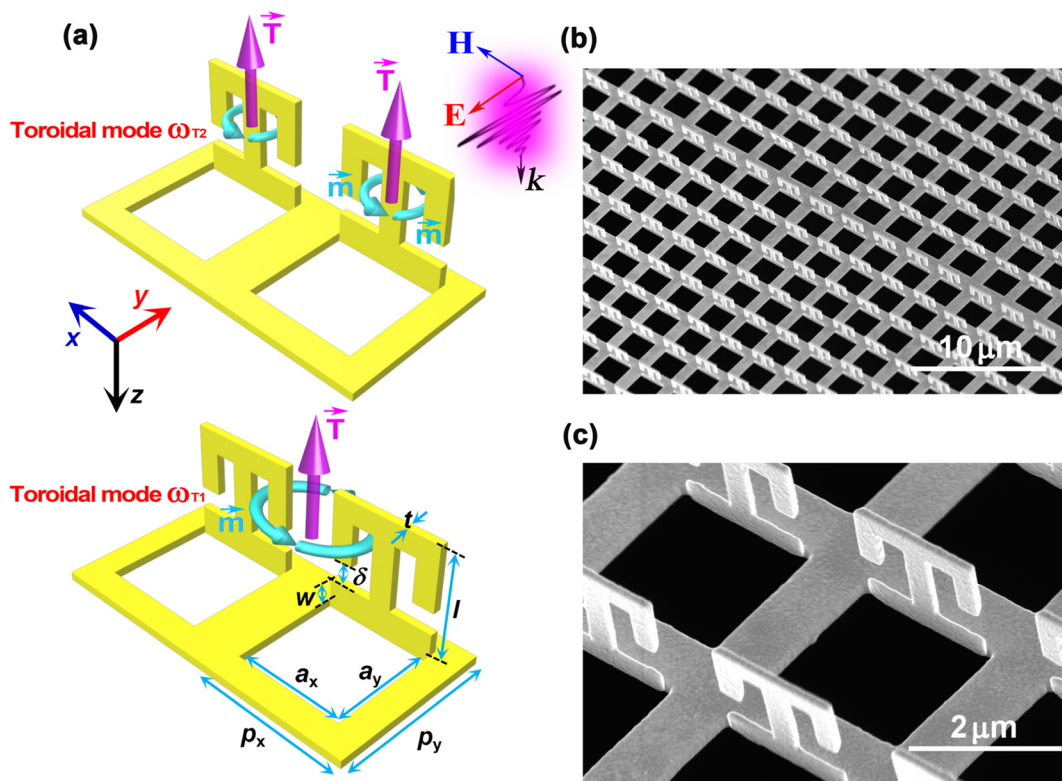


Figure 1. Design of 3D toroidal metamaterials. (a) Schematic of toroidal dipole modes generated due to circulating magnetic field produced by current loops, as well as the schematic illustration of 3D toroidal metamaterial; cyan and purple arrows depict the direction of magnetic and toroidal moment, respectively. The geometrical parameters depicted in the schematic configuration are $a_x = a_y = 2 \mu\text{m}$, $l = 1.98 \mu\text{m}$, $w = 400 \text{ nm}$, and $\delta = 500 \text{ nm}$; Periodicity of the structure array is $p_x = p_y = 3 \mu\text{m}$, and thickness of the gold film is $t = 150 \text{ nm}$, respectively. (b) SEM image of the fabricated 3D toroidal metamaterials. (c) A magnified view of the 3D structures.

toroidal dipolar responses by artificial composites is an emerging field that is worth extensive exploration.

Metamaterials, composite arrays of artificial subwavelength structures, have attracted enormous attention in the scientific community over the last two decades due to their novel physical phenomena and remarkable functionalities, which are not available in natural materials, such as negative refractive index,¹² invisibility cloaking,^{13,14} plasmon-induced transparency,^{15,16} and superlenses.¹⁷ The exotic electromagnetic response in metamaterials is achieved by properly designing and tailoring the geometry of the metamaterial elements to resonantly excite oscillating charges or loop currents, which usually involves the concept of electric and magnetic multipole excitations. Recently, dynamic toroidal multipoles, the third family of electromagnetic multipoles which are necessary for the complete multipole analysis of an arbitrary radiating source, have been observed in metamaterials, providing a platform to unveil the associated intriguing optical phenomena. In 2010, toroidal dipolar resonance was experimentally demonstrated in the microwave regime with an elaborate complex 3D electromagnetic metamaterial composed of multifold split-ring resonators with toroidal topology.¹⁸ Subsequently, the toroidal metamaterial was extended to the infrared wavelengths by scaling down the size of split-ring resonators.^{19,20} Since then enormous efforts have been made to explore many exotic electromagnetic phenomena associated with the toroidal multipoles in artificial media,^{21–26} such as resonant transparency,^{27,28} anomalous optical activity,²⁹ enhanced optical force,^{30,31} all-optical Hall effect,³² and lasing spaser.³³ In addition, it has been shown that the interaction between a

toroidal mode and other multipole could result in many appealing phenomena. For example, due to the identical radiation pattern of a toroidal dipole and an electric dipole in the far field, a toroidal dipole interacting with an electric dipole may exhibit nonradiating characteristics, which can be regarded as a nontrivial anapole.^{34,35}

Thus far, all preceding studies have exclusively focused on a single toroidal dipole resonance,^{18–40} whereas simultaneous excitation of multiple toroidal dipole modes has not hitherto been explored. Thus, it should be of great interest to explore new methods to achieve double or even multiple toroidal dipole responses, which has direct analogy to the toroidal states in the condensed matter systems. This will not only promote the understanding of toroidal moments in condensed matter physics, but also be very useful in investigating other physical (optical, acoustic) phenomena involving the multiple toroidal states. In addition, metamaterials that manifest strong toroidal response has the ability to enhance electromagnetic field confinement by squeezing time varying magnetic field into a small circular region. Due to the very weak coupling to free space and high electromagnetic energy confinement, metamaterials supporting toroidal dipole play an important role in boosting light-matter interaction and energy transfer at subwavelength scale. However, as the resonant frequency increases to infrared and visible regime, the realization of a toroidal response in true 3D sophisticated metamaterials becomes extremely difficult due to the limitations of fabrication, which makes it very difficult to experimentally explore the elusive optical phenomena involving the toroidal moment. Although certain advances have been achieved in the

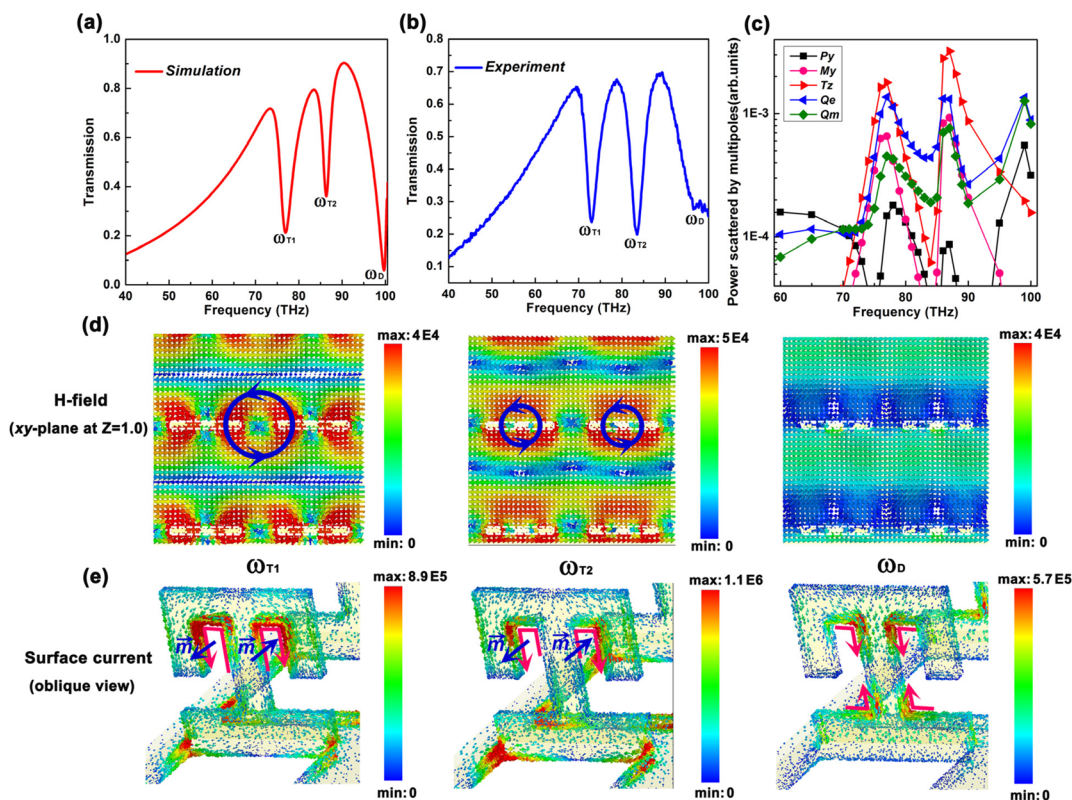


Figure 2. Toroidal responses of the 3D metamaterial. (a) The simulated and (b) measured transmission spectra of the 3D toroidal metamaterial for a y -polarized wave at normal incidence. (c) Dispersion of scattered power for various multipole moments induced in the metamaterial. (d) The simulated magnetic field (on xy -plane at $z = 1.0 \mu\text{m}$) distributions of four unit cell of the toroidal metamaterials. Note that the white dashed frames in the H -field maps marked the positions of vertical JDSRRs, and blue circle indicate the magnetic field vortices. (e) Surface current distributions and magnetic dipole orientation on one unit-cell of the metamaterials at respective resonances.

implementation of toroidal resonance in planar metamaterials, simultaneously achieving multiple toroidal resonances in metamaterials is still extremely challenging and remains formidable task due to lack of available routes to excite and control them.

In this Letter, we experimentally demonstrate, for the first time to the best of our knowledge, multiple strong toroidal dipole resonances via surface-plasmon-polariton (SPP) excitation in a 3D metamaterial operating at infrared frequencies. The 3D toroidal metamaterials consist of an array of subwavelength joint double split ring resonators (JDSRRs) and square apertures arranged in a square lattice geometry. The toroidal resonances are induced by coupling between the bright SPP mode supported by the aperture array and dark inductive-capacitive resonant modes of the out-of-plane JDSRRs. The lateral coupling between adjacent unit-cells results in an otherwise inaccessible brand new hybridized toroidal dipolar mode. Field distributions clearly manifest the existence of toroidal mode with tightly confined magnetic vortex in the subwavelength 3D structures. Because of the unique field configuration of the coupled toroidal modes, the proposed 3D metamaterial exhibiting sharp toroidal resonances may have broad applications in low Joule loss quantum plasmonics, tunable absorbers, low-threshold plasmonic lasing, nonlinear processing, and chemical/biological sensing.

RESULTS AND DISCUSSION

Our toroidal metamaterial comprises two conductively joint gold SRRs, merged to form a single enlarged JDSRR with two

split gaps, standing on the edge of a square aperture on an ultrathin self-supporting gold membrane, as shown in Figure 1a. For a plane wave polarized in the y -direction at normal incidence, the periodic square apertures function as a 2D grating which compensates the momentum difference between propagating photons and plasmons, and therefore enables the excitation of SPPs at the metal-air interface, resulting in an extraordinary optical transmission (EOT).^{41–45} Through a conductively coupling between the square aperture and vertical JDSRR, the inductive-capacitive (LC) resonance^{39,40,46,47} in each SRR can be excited with the currents in the two loops of each SRR oscillating out of phase, such that their magnetic moment vectors pointing in the opposite directions perpendicular to the JDSRR surface. This results in head-to-tail configuration of the magnetic moments of nearby SRRs, which is responsible for the excitation of the toroidal resonance modes. Because of the indirect excitation of the JDSRR, this 3D metamaterial results in a suppressed electric and enhanced toroidal dipole response. Intriguingly, due to the fact that the induced magnetic dipole excitation in the adjacent resonator are always in opposite direction, the 3D metamaterial can support a unique hybridized toroidal mode in which the adjacent unit cells are strongly coupled (see Figure 1a).

The qualitative arguments represented above are fully supported by numerical simulations performed using a full three-dimensional Maxwell equations solver based on the finite element method with periodic boundary conditions. Calculated densities of the induced electrical currents are used to compute the scattered power of the resonantly excited electric and

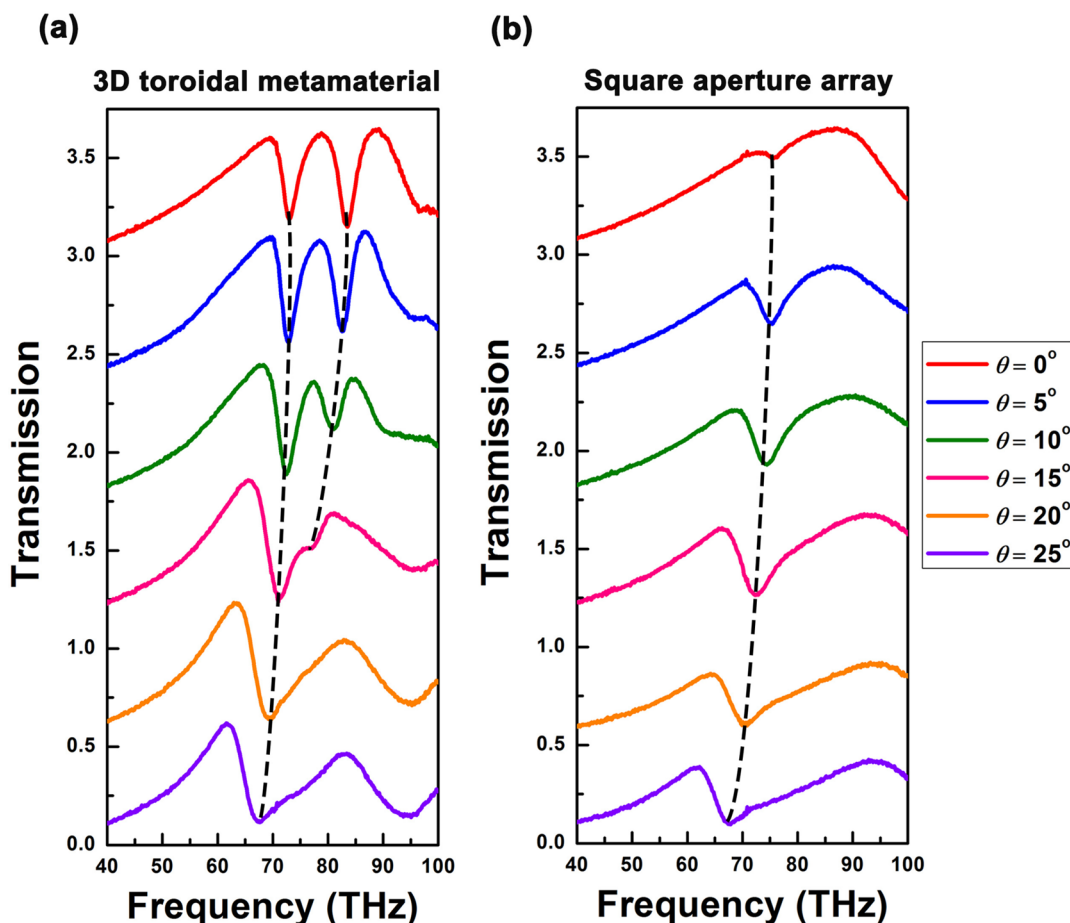


Figure 3. Experimental measured transmission spectra of the 3D toroidal metamaterial and square aperture array at different incident angles. (a) Transmission spectra of the 3D toroidal metamaterial for TM-polarized incident electromagnetic wave when sweeping the incident angle. Spectra were taken every 5° from $\theta = 0^\circ$ to $\theta = 25^\circ$, respectively. (b) Transmission spectra of the square aperture array with different values of incident angle under TM-polarized excitation. An arbitrary offset was added to each data to separate them in the figure for clarity.

magnetic multipoles, as well as the toroidal dipole of the 3D metamaterial. The fabrication method of 3D folding metamaterials is based on the focused ion beam (FIB) stress-induced deformation technique⁴⁸ on self-supported gold nanofilm, and a detailed description of the fabrication process is provided in the Supporting Information. Figure 1b,c shows the scanning electron microscope (SEM) images of as-fabricated 3D metamaterial array in which high quality and good uniformity of the structures are clearly observed. Subsequently, a Fourier transform infrared (FTIR) spectrometer is used to measure the transmission spectra in the infrared region.

Figure 2a,b depict the simulated and measured transmission spectra of metamaterial samples with y -polarized incident electromagnetic wave. Three distinct resonant dips appear in the background spectrum of a broadband EOT profile. Excitations of two toroidal modes at $\omega_{T1} = 73$ THz and $\omega_{T2} = 83.5$ THz are clearly observed in the experimentally measured transmission spectra. The quality factor (Q factor), defined as the ratio of resonance frequency to the full width at half-maximum, for the measured resonance at ω_{T1} and ω_{T2} reach 24 and 26, respectively. Those values are much higher than that of dipole resonance supported by the conventional metamaterials (Q factor less than 10).^{39,40,46,47} In order to study the resonances of metamaterial quantitatively, the multipole moments are calculated from the induced volume current

density in the 3D metamaterial,^{2,18} with the extracted multipole scattering intensities shown in Figure 2c. In our 3D metamaterial, only the electric/magnetic dipole, electric/magnetic quadrupole, and toroidal dipole provide significant contributions to the metamaterial responses, while all the other higher order multipoles are very weak and therefore can be neglected. Although electric and magnetic quadrupole moments are also resonant at the two resonance frequencies, the intensity of toroidal component (T_z) at resonance ω_{T1} and ω_{T2} is much stronger than that of electric quadrupole moment (Q_e) and over 1 order of magnitude stronger than that of electric dipole (P_y), respectively. Here it should be noted that the strong toroidal component (T_z) does not contribute directly to the far-field radiation (transmission spectrum) at normal incidence (incident angle $\theta = 0^\circ$), but indirectly through the mediation of the SPP mode. On the other hand, the net electric dipole moment and, consequently, the radiative losses are dramatically reduced, resulting in very large Q factor of the two resonances.^{27,46} However, the toroidal moments can contribute to scattering significantly once the light is incident at oblique direction, which will be discussed later.

To clarify the underlying physical mechanism of the generated resonant modes, the magnetic field and current distributions at the resonance frequencies are plotted in Figure 2d and e, respectively. Interestingly, at the low frequency toroidal resonance ω_{T1} , a strong magnetic vortex appears to

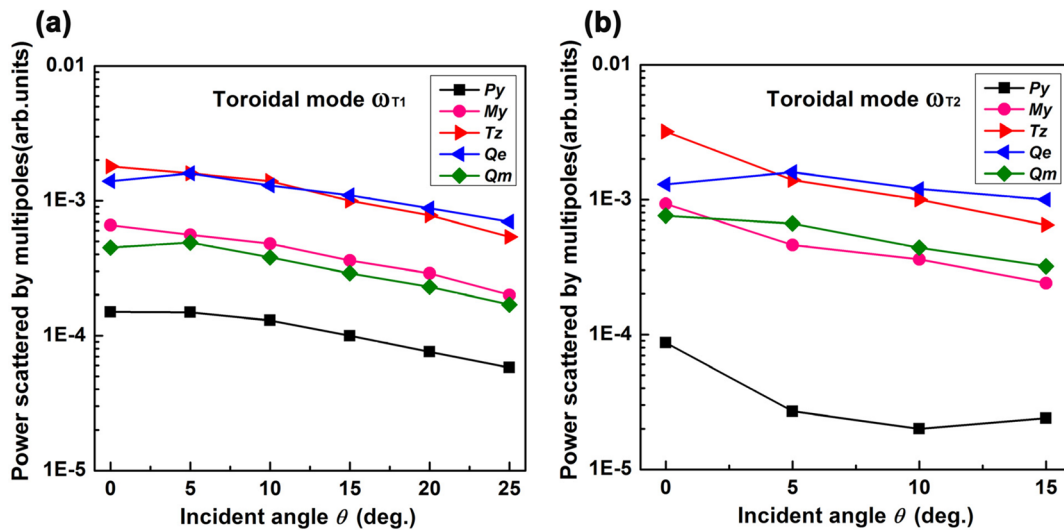


Figure 4. Magnitude of excited multipole components at two toroidal resonances (a) ω_{T1} and (b) ω_{T2} as a function of incident angle. Note that five most dominant multipole components (toroidal dipole, electric dipole, magnetic dipole, electric quadrupole, and magnetic quadrupole) that contribute to the resonant responses of the metamaterial are presented.

connect the adjacent JDSRR rather than within the JDSRR itself. This toroidal resonance in the 3D metamaterials originates from the near-field interactions between the adjacent JDSRRs in x -direction, which results in tight confinement of the magnetic field to form a magnetic vortex. Figure 2e displays the configuration of the surface current distribution in the JDSRR, which shows that the loop currents and consequently the magnetic dipoles in the left part of the unit cell and right part of the neighboring one are opposite to each other. This head-to-tail configuration of magnetic dipole result in strong coupling between the neighboring JDSRRs mediated by the circulating magnetic fields that form the magnetic field vortices. This circulating magnetic field concentrated in subwavelength region generates toroidal dipolar excitation oriented along the z -axis. It is worth mentioning that the currents in the vertical JDSRRs generating the toroidal dipole moment do not radiate into the far field since only currents that are parallel to the external electric field can contribute to the far-field radiation.^{18,46} Therefore, this toroidal resonance drastically suppresses the radiation losses and couples weakly to free space, which result in strongly confined photon energy in the metamaterial and enhances the Q factor.

At the higher frequency toroidal resonance ω_{T2} , the calculated magnetic field are observed to form magnetic vortices that are tightly concentrated within the individual unit-cell, as shown in Figure 2d. The induced currents also form circulating surface currents along each SRR, giving rise to a magnetic dipole which points in forward or backward direction perpendicular to the JDSRR plane. Opposite circular currents in the left and right constituent SRRs of each JDSRR generate a circular magnetic moment distribution that is perpendicular to the JDSRR surface, giving rise to a strong toroidal moment pointing in the z -direction. The large amount of magnetic energy trapped in the 3D metamaterial leads to the enhancement of Q factor of toroidal resonance as a consequence of strongly suppressed electric dipole moment and radiative losses (see Figure 2c,d). Besides, the resonance ω_D , appearing near the first-order diffraction mode,⁴⁶ is dominated by the magnetic quadrupole moment (Q_m) and electric quadrupole moment (Q_e). In contrast, there is no magnetic vortex appearing in the

magnetic field plot, thus the toroidal component is very weak at this resonance.

To further substantiate the concept of SPP mediated toroidal responses, we perform experimental measurement of the transmission spectra both for the 3D metamaterial and a sample consisting of square aperture array only at different incident angles, as shown in Figure 3a and b, respectively. For the 3D metamaterial, as the angle of incidence is increased, both the two toroidal resonances exhibit a redshift due to the spatial dispersion of the 3D metamaterial. Moreover, the resonance of the higher frequency toroidal mode becomes gradually weakened with increasing incident angle. Here it is worth noting that the contribution of the strong toroidal moment to the far-field radiation (transmission spectrum) increases gradually as the incident angle increases.²⁰ On the other hand, for the sample of square aperture array, an initially broadband EOT peak at normal incidence gradually split into two separated peaks at increased incident angle, as depicted in Figure 3b. The dependence of the spectra of the 3D metamaterial over incident angle can be well explained based on the angle dependent momentum matching condition. For a square aperture array, SPPs are excited at the metal–air interface when their momentum matches the momentum of the incident photon and obeys conservation of momentum

$$\vec{k}_{\text{spp}} = \vec{k} \sin \theta \pm i\vec{G}_x \pm j\vec{G}_y \quad (1)$$

where \vec{k}_{spp} is the surface plasmon wave vector, θ is the incident angle, \vec{G}_x and \vec{G}_y are the reciprocal lattice vectors for a square lattice with $|\vec{G}_x| = |\vec{G}_y| = 2\pi/p$, and i, j are integers. In the case of normal incidence ($\theta = 0^\circ$), the component of the incident photon's wave vector in the square aperture plane is zero, and the SPP vector is only provided by the reciprocal lattice vectors of the square lattice, which couples with the vertical JDSRR resulting in two toroidal resonances on a broadband EOT peak. By increasing the incident angle from $\theta = 0^\circ$ to $\theta = 25^\circ$, the incident light excites different SPP modes ($\vec{k} \sin \theta + \vec{G}_x$, $\vec{k} \sin \theta - \vec{G}_y$), and therefore, the EOT peak of the SPP mode is gradually split into two peaks shifting toward opposite directions. The mismatch between the SPP mode and toroidal modes result in the degradation of the toroidal responses within

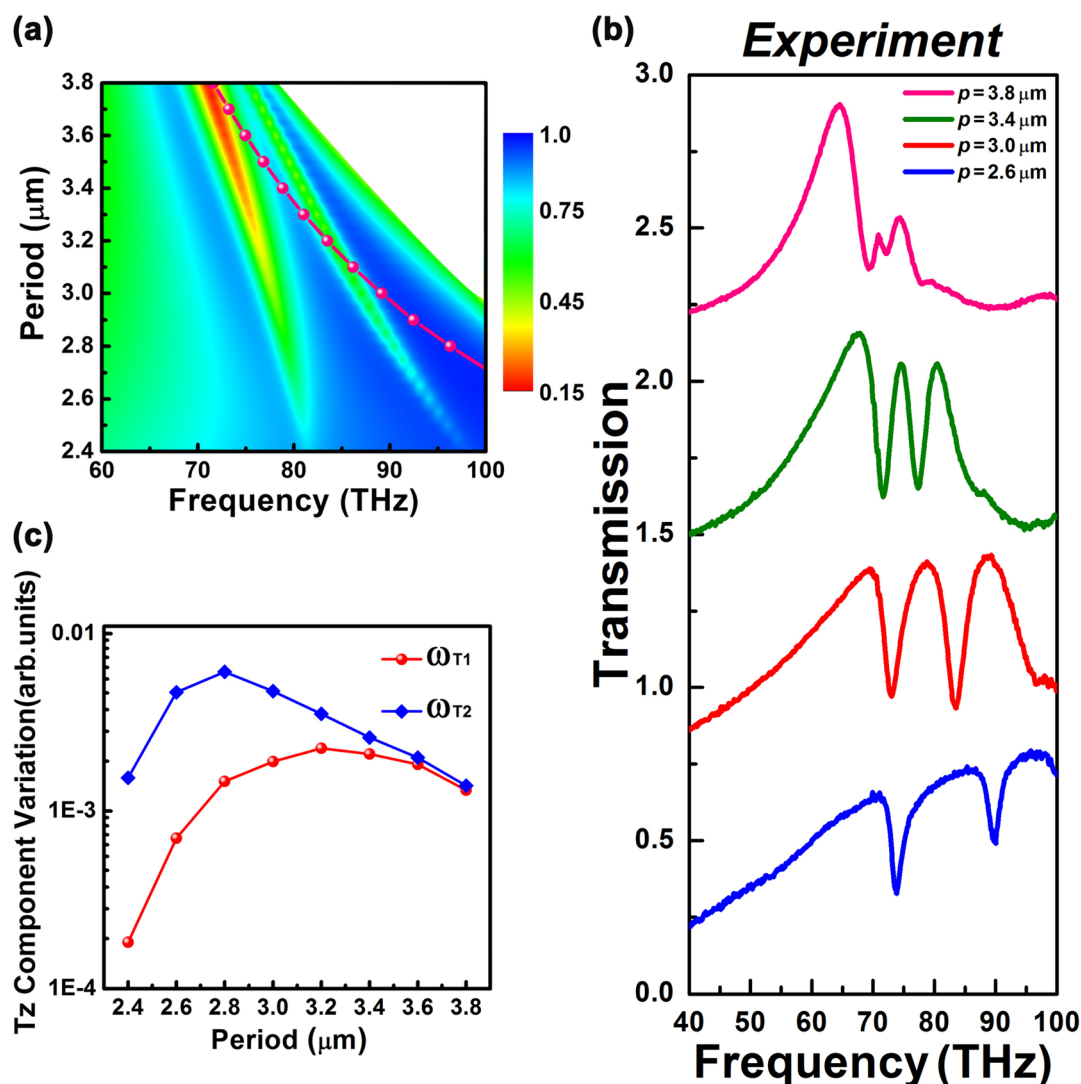


Figure 5. Dependence of toroidal resonances over periodicity. (a) Calculated transmission spectra of the 3D toroidal MM with different values of period (p) under y -polarized excitation. Color bar indicates transmission from 0.15 (red) to 1 (blue). The dotted red curve overlapped on the transmission spectra is calculated energy dispersion of surface plasmons. Higher-order modes above the first-order diffraction mode are blocked by white triangle to focus on the toroidal modes. (b) Experimental measured transmission spectra of the 3D toroidal metamaterials with period varied from 2.6 to 3.8 μm in 0.4 μm increments. (c) Magnitude of excited toroidal dipole component as a function of period, at the instant of the electromagnetic resonance.

the transmission valley between the two EOT peaks. When the angle of incidence θ is larger than the critical point ($\theta \sim 15^\circ$), the detuning is so large that the coupling between the SPP mode and toroidal modes is diminished, resulting in the vanishing of the higher frequency toroidal mode and weaken of the lower frequency toroidal response. It is worth mentioning that, due to the Wood's anomalies,^{41–44} a broad transmission dip appears in-between the two split EOT peaks, which overlaps with the lower frequency toroidal mode as the incident angle increases. Meanwhile, the T_z component of the lower frequency toroidal resonance is gradually attenuated (see Supporting Information, Figure S3).

To better visualize the contribution of multipole components at oblique incidence, the magnitudes of multipole components at the two resonance frequencies as a function of the incident angle are retrieved, as shown in Figure 4. For the lower frequency toroidal mode (ω_{T1}), the toroidal moment monotonically decreases with the increase of incident angle, and both the toroidal dipole and electric quadrupole moments

dominate all other multipoles, as shown in Figure 4a. In this case, besides the radiation mediated by SPP, the toroidal dipole also directly radiates into the far field. The magnitudes of the electric and magnetic quadrupole slightly enhanced at small incident angle due to the direct excitation of the JDSRR by TM-polarized light. Furthermore, the intensity of all the multiple components gradually diminishes as the incident angle of light become very large because of the low coupling efficiency of the SPP mode to the free space radiation due to the momentum mismatch. It is observed that the toroidal dipole moment of the higher frequency resonance (ω_{T2}) also gradually decrease in intensity and both the toroidal and electric quadrupole play dominant roles until the resonance disappear at higher incident angle (see Figure 4b). Therefore, by simply tuning the incident angle, the contribution of the toroidal moment to the radiation properties of the metamaterials can be readily manipulated, and the number of the toroidal mode can be controlled.

The toroidal responses can be further optimized by choosing an appropriate periodicity (p). Figure 5a and b show the calculated and experimentally measured transmission spectra of the 3D toroidal metamaterials, respectively, which exhibit a strong dependence on the periodicity of the apertures, since the periodicity determines the resonant frequencies of the EOT peaks.^{40–44} The position of the EOT peaks as a function of periodicity can be approximated by the surface plasmon dispersion for a smooth film,^{41–43}

$$f_{\text{sp}} = c(i^2 + j^2)^{1/2}/p \left(\frac{\epsilon_{\text{air}}\epsilon_{\text{gold}}}{\epsilon_{\text{air}} + \epsilon_{\text{gold}}} \right)^{1/2} \quad (2)$$

where c is the speed of the electromagnetic wave, ϵ_{air} is the dielectric constant of the air, and ϵ_{gold} is that of the gold. With the increase of the periodicity p from 2.4 to 3.8 μm , the (0,1) mode of the EOT is red-shifted, consequently resulting in the spectrally redshift of both toroidal modes as depicted in Figure 5a. The experimental results in Figure 5b show that both toroidal modes experience a redshift and modulation in resonant intensities, which is consistent with the calculated data. The strong dependence of the toroidal modes over the resonant frequency of the EOT peak further confirms that the toroidal modes strongly couple to the SPP excitation. In essence, the excitation intensities of both toroidal modes strongly depend on the frequency of the EOT peak, which become more prominent as the frequencies of those modes are in proximity to that of the EOT peak (see Figure 5a) due to the enhanced coupling efficiency.

The z -component of the toroidal dipole (T_z) excitation for the 3D metamaterial with different values of period (p) is extracted and shown in Figure 5c. The optimal period for toroidal mode ω_{T1} and ω_{T2} are around 3.2 and 2.8 μm , respectively. For the periodicity above the optimized values, the z -component of the toroidal dipole (T_z) for both toroidal resonances decreases monotonically due to the diminished coupling strength of the adjacent JDSRRs and mismatch between SPP mode and toroidal mode. Consequently, the two resonance ω_{T1} and ω_{T2} are dominated by electric and magnetic multipoles (not shown here). When the periodicity is decreased below the optima, although the coupling effect of the adjacent JDSRRs is enhanced by decreasing the distance, the intensity of the toroidal resonance decreases gradually due to the weak excitation efficiency (the frequency deviations between the toroidal resonances and EOT peak are too large). For instance, in the case of $p = 2.4 \mu\text{m}$, the detuning between the toroidal modes and EOT peak is so large that the coupling between the toroidal modes and SPP mode is very weak, which result in fading of the toroidal modes. All of the above observations indicate that beside the intrinsic toroidal responses generated by the JDSRRs, the lattice periodicity plays a key role by modifying the cell–cell coupling and controlling the excited SPP mode. Therefore, judiciously choosing the periodicity would help optimize the resonance properties of the 3D metamaterial.

CONCLUSIONS

In summary, we have experimentally demonstrated a novel 3D metamaterial that supports SPP-mediated double high Q -factor toroidal resonances. Our design exploits the strong coupling between the square aperture array and JDSRRs to produce narrow toroidal resonances emerging from the EOT back-

ground with Q factors exceeding 20 at infrared regime. Due to the unique topology of the toroidal modes and tightly confined electromagnetic field, the toroidal metamaterial allows spatially large field enhancement at subwavelength scale, which can be utilized to enhancing light–matter interaction and energy transfer. The concept of SPP induced multiple toroidal resonances provide a new avenue for designing the next generation ultrasensitive sensor, narrow-band filter, modulator, and coherent lasing spaser. Furthermore, it may also advance the understanding of the physical mechanism of the widespread light–matter and intermolecular interactions associated with toroidal states in nature.

ASSOCIATED CONTENT

Supporting Information

The Supporting Information is available free of charge on the ACS Publications website at DOI: 10.1021/acsp Photonics.7b00529.

Detailed fabrication method, numerical simulation information, and additional figures (PDF).

AUTHOR INFORMATION

Corresponding Authors

*E-mail: s.zhang@bham.ac.uk.

*E-mail: jjli@iphy.ac.cn.

*E-mail: czgu@iphy.ac.cn.

ORCID

Shuang Zhang: 0000-0003-4556-2333

Junjie Li: 0000-0002-1508-9891

Author Contributions

S.Y. and S.Z. conceived the idea and designed the experiment; S.Y., L.J., and W.L. fabricated the samples; S.Y. and Z.L. performed the optical measurements; S.Y. and Z.L. conducted the calculations and simulations; S.Y. and S.Z. prepared the manuscript. S.Z., J.L., and C.G. supervised the overall project. All the authors analyzed the data and discussed the results.

Notes

The authors declare no competing financial interest.

ACKNOWLEDGMENTS

S.Y. would like to thank Professor Nikolay I. Zheludev and Professor J. R. Sun for valuable discussions. This work is supported by the National Key Research and Development Program of China under Grant No. 2016YFA0200400, and No. 2016YFA0200800; the National Natural Science Foundation of China under Grants Nos. 91323304, 11674387, 11504414, 11574369, 11574385, 11574368, and 61390503; Strategic Priority Research Program of the Chinese Academy of Sciences under Grant No. XDB07020200; European Research Council Consolidator Grant (TOPOLOGICAL).

REFERENCES

- (1) Zel'dovich, Y. B. The relation between decay asymmetry and dipole moment of elementary particles. *Sov. Phys. JETP* **1958**, *6*, 1184.
- (2) Dubovik, V. M.; Tugushev, V. V. Toroid moments in electrostatics and solid-state physics. *Phys. Rep.* **1990**, *187*, 145–202.
- (3) Ceulemans, A.; Chibotaru, L. F.; Fowler, P. W. Molecular anapole moments. *Phys. Rev. Lett.* **1998**, *80*, 1861.
- (4) Naumov, I. I.; Bellaiche, L.; Fu, H. Unusual phase transitions in ferroelectric nanodisks and nanorods. *Nature* **2004**, *432*, 737–740.

- (5) Sawada, K.; Nagaosa, N. Optical magnetoelectric effect in multiferroic materials: Evidence for a Lorentz force acting on a ray of light. *Phys. Rev. Lett.* **2005**, *95*, 237402.
- (6) Van Aken, B. B.; Rivera, J. P.; Schmid, H.; Fiebig, M. Observation of ferrotoroidic domains. *Nature* **2007**, *449*, 702–705.
- (7) Spaldin, N. A.; Fiebig, M.; Mostovoy, M. The toroidal moment in condensed-matter physics and its relation to the magnetoelectric effect. *J. Phys.: Condens. Matter* **2008**, *20*, 434203.
- (8) Zvezdin, A. K.; Kostyuchenko, V. V.; Popov, A. I.; Popkov, A. F.; Ceulemans, A. Toroidal moment in the molecular magnet V15. *Phys. Rev. B: Condens. Matter Mater. Phys.* **2009**, *80*, 172404.
- (9) Thorner, G.; Kiat, J. M.; Bogicevic, C.; Kornev, I. Axial hypertoroidal moment in a ferroelectric nanotorus: A way to switch local polarization. *Phys. Rev. B: Condens. Matter Mater. Phys.* **2014**, *89*, 220103.
- (10) Kezsmarki, I.; Kida, N.; Murakawa, H.; Bordacs, S.; Onose, Y.; Tokura, Y. Enhanced directional dichroism of terahertz light in resonance with magnetic excitations of the multiferroic $\text{Ba}_2\text{CoGe}_2\text{O}_7$ oxide compound. *Phys. Rev. Lett.* **2011**, *106*, 057403.
- (11) Zimmermann, A. S.; Meier, D.; Fiebig, M. Ferroic nature of magnetic toroidal order. *Nat. Commun.* **2014**, *5*, 4796.
- (12) Valentine, J.; Zhang, S.; Zentgraf, T.; Ulin-Avila, E.; Genov, D. A.; Bartal, G.; Zhang, X. Three-dimensional optical metamaterial with a negative refractive index. *Nature* **2008**, *455*, 376–379.
- (13) Schurig, D.; Mock, J. J.; Justice, B. J.; Cummer, S. A.; Pendry, J. B.; Starr, A. F.; Smith, D. R. Metamaterial electromagnetic cloak at microwave frequencies. *Science* **2006**, *314*, 977–980.
- (14) Ergin, T.; Stenger, N.; Brenner, P.; Pendry, J. B.; Wegener, M. Three-dimensional invisibility cloak at optical wavelengths. *Science* **2010**, *328*, 337–339.
- (15) Zhang, S.; Genov, D. A.; Wang, Y.; Liu, M.; Zhang, X. Plasmon-induced transparency in metamaterials. *Phys. Rev. Lett.* **2008**, *101*, 047401.
- (16) Yang, S.; Xia, X.; Liu, Z.; Yiwen, E.; Wang, Y.; Tang, C.; Li, W.; Li, J.; Wang, L.; Gu, C. Multispectral plasmon-induced transparency in hyperfine terahertz meta-molecules. *J. Phys.: Condens. Matter* **2016**, *28*, 445002.
- (17) Zhang, X.; Liu, Z. Superlenses to overcome the diffraction limit. *Nat. Mater.* **2008**, *7*, 435–441.
- (18) Kaelberer, T.; Fedotov, V. A.; Papasimakis, N.; Tsai, D. P.; Zheludev, N. I. Toroidal dipolar response in a metamaterial. *Science* **2010**, *330*, 1510–1512.
- (19) Huang, Y. W.; Chen, W. T.; Wu, P. C.; Fedotov, V.; Savinov, V.; Ho, Y. Z.; Chau, Y. F.; Zheludev, N. I.; Tsai, D. P. Design of plasmonic toroidal metamaterials at optical frequencies. *Opt. Express* **2012**, *20*, 1760–1768.
- (20) Liu, Z.; Du, S.; Cui, A.; Li, Z.; Fan, Y.; Chen, S.; Li, W.; Li, J.; Gu, C. High-quality-factor mid-infrared toroidal excitation in folded 3D metamaterials. *Adv. Mater.* **2017**, *29*, 1606298.
- (21) Papasimakis, N.; Fedotov, V. A.; Savinov, V.; Raybould, T. A.; Zheludev, N. I. Electromagnetic toroidal excitations in matter and free space. *Nat. Mater.* **2016**, *15*, 263–271.
- (22) Ögüt, B.; Talebi, N.; Vogelgesang, R.; Sigle, W.; van Aken, P. A. Toroidal plasmonic eigenmodes in oligomer nanocavities for the visible. *Nano Lett.* **2012**, *12*, 5239–5244.
- (23) Dong, Z. G.; Ni, P.; Zhu, J.; Yin, X.; Zhang, X. Toroidal dipole response in a multifold double ring metamaterial. *Opt. Express* **2012**, *20*, 13065–13070.
- (24) Savinov, V.; Fedotov, V. A.; Zheludev, N. I. Toroidal dipolar excitation and macroscopic electromagnetic properties of metamaterials. *Phys. Rev. B: Condens. Matter Mater. Phys.* **2014**, *89*, 205112.
- (25) Basharin, A. A.; Kafesaki, M.; Economou, E. N.; Soukoulis, C. M.; Fedotov, V. A.; Savinov, V.; Zheludev, N. I. Dielectric metamaterials with toroidal dipolar response. *Phys. Rev. X* **2015**, *5*, 011036.
- (26) Watson, D. W.; Jenkins, S. D.; Ruostekoski, J.; Fedotov, V. A.; Zheludev, N. I. Toroidal dipole excitations in metamolecules formed by interacting plasmonic nanorods. *Phys. Rev. B: Condens. Matter Mater. Phys.* **2016**, *93*, 125420.
- (27) Fedotov, V. A.; Rogacheva, A. V.; Savinov, V.; Tsai, D. P.; Zheludev, N. I. Resonant transparency and non-trivial non-radiating excitations in toroidal metamaterials. *Sci. Rep.* **2013**, *3*, 2967.
- (28) Liu, W.; Zhang, J.; Miroshnichenko, A. E. Toroidal dipole-induced transparency in core-shell nanoparticles. *Laser Photonics Rev.* **2015**, *9*, 564–570.
- (29) Raybould, T. A.; Fedotov, V. A.; Papasimakis, N.; Kuprov, I.; Youngs, I. J.; Chen, W. T.; Tsai, D. P.; Zheludev, N. I. Toroidal circular dichroism. *Phys. Rev. B: Condens. Matter Mater. Phys.* **2016**, *94*, 035119.
- (30) Zhang, X. L.; Wang, S. B.; Lin, Z. F.; Sun, H. B.; Chan, C. T. Optical force on toroidal nanostructures: Toroidal dipole versus renormalized electric dipole. *Phys. Rev. A: At, Mol., Opt. Phys.* **2015**, *92*, 043804.
- (31) Jin, R. C.; Li, J.; Wang, Y. H.; Zhu, M. J.; Li, J. Q.; Dong, Z. G. Optical force enhancement and annular trapping by plasmonic toroidal resonance in a double-disk metastructure. *Opt. Express* **2016**, *24*, 27563–27568.
- (32) Dong, Z. G.; Zhu, J.; Yin, X.; Li, J.; Lu, C.; Zhang, X. All-optical Hall effect by the dynamic toroidal moment in a cavity-based metamaterial. *Phys. Rev. B: Condens. Matter Mater. Phys.* **2013**, *87*, 245429.
- (33) Huang, Y. W.; Chen, W. T.; Wu, P. C.; Fedotov, V. A.; Zheludev, N. I.; Tsai, D. P. Toroidal lasing spaser. *Sci. Rep.* **2013**, *3*, 1237.
- (34) Miroshnichenko, A. E.; Evlyukhin, A. B.; Yu, Y. F.; Bakker, R. M.; Chipouline, A.; Kuznetsov, A. I.; Luk'yanchuk, B.; Chichkov, B. N.; Kivshar, Y. S. Nonradiating anapole modes in dielectric nanoparticles. *Nat. Commun.* **2015**, *6*, 8069.
- (35) Basharin, A. A.; Chuguevsky, V.; Volsky, N.; Kafesaki, M.; Economou, E. N. Extremely high Q-factor metamaterials due to anapole excitation. *Phys. Rev. B: Condens. Matter Mater. Phys.* **2017**, *95*, 035104.
- (36) Dong, Z. G.; Zhu, J.; Rho, J.; Li, J. Q.; Lu, C.; Yin, X.; Zhang, X. Optical toroidal dipolar response by an asymmetric double-bar metamaterial. *Appl. Phys. Lett.* **2012**, *101*, 144105.
- (37) Fan, Y.; Wei, Z.; Li, H.; Chen, H.; Soukoulis, C. Low-loss and high-Q planar metamaterial with toroidal moment. *Phys. Rev. B: Condens. Matter Mater. Phys.* **2013**, *87*, 115417.
- (38) Bao, Y.; Zhu, X.; Fang, Z. Plasmonic toroidal dipolar response under radially polarized excitation. *Sci. Rep.* **2015**, *5*, 11793.
- (39) Gupta, M.; Savinov, V.; Xu, N.; Cong, L.; Dayal, G.; Wang, S.; Zhang, W.; Zheludev, N. I.; Singh, R. Sharp toroidal resonances in planar terahertz metasurfaces. *Adv. Mater.* **2016**, *28*, 8206–8211.
- (40) Gupta, M.; Singh, R. Toroidal versus Fano resonances in high Q planar THz metamaterials. *Adv. Opt. Mater.* **2016**, *4*, 2119–2125.
- (41) Ghaemi, H. F.; Thio, T.; Grupp, D. E.; Ebbesen, T. W.; Lezec, H. J. Surface plasmons enhance optical transmission through subwavelength holes. *Phys. Rev. B: Condens. Matter Mater. Phys.* **1998**, *58*, 6779.
- (42) Ebbesen, T. W.; Lezec, H. J.; Ghaemi, H. F.; Thio, T.; Wolff, P. A. Extraordinary optical transmission through sub-wavelength hole arrays. *Nature* **1998**, *391*, 667–669.
- (43) Martín-Moreno, L.; García-Vidal, F. J.; Lezec, H. J.; Pellerin, K. M.; Thio, T.; Pendry, J. B.; Ebbesen, T. W. Theory of extraordinary optical transmission through subwavelength hole arrays. *Phys. Rev. Lett.* **2001**, *86*, 1114.
- (44) Fan, W.; Zhang, S.; Minhas, B.; Malloy, K. J.; Brueck, S. R. J. Enhanced infrared transmission through subwavelength coaxial metallic arrays. *Phys. Rev. Lett.* **2005**, *94*, 033902.
- (45) Liu, H.; Lalanne, P. Microscopic theory of the extraordinary optical transmission. *Nature* **2008**, *452*, 728–731.
- (46) Yang, S.; Liu, Z.; Xia, X.; E, Y.; Tang, C.; Wang, Y.; Li, J.; Wang, L.; Gu, C. Excitation of ultrasharp trapped-mode resonances in mirror-symmetric metamaterials. *Phys. Rev. B: Condens. Matter Mater. Phys.* **2016**, *93*, 235407.
- (47) Yang, S.; Tang, C.; Liu, Z.; Wang, B.; Wang, C.; Li, J.; Wang, L.; Gu, C. Simultaneous excitation of extremely high-Q-factor trapped and

octupolar modes in terahertz metamaterials. *Opt. Express* **2017**, *25*, 15938–15946.

(48) Cui, A.; Liu, Z.; Li, J.; Shen, T. H.; Xia, X.; Li, Z.; Gong, Z.; Li, H.; Wang, B.; Li, J.; Yang, H.; Li, W.; Gu, C. Directly patterned substrate-free plasmonic ‘nanograter’ structures with unusual Fano resonances. *Light: Sci. Appl.* **2015**, *4*, e308.